CHAPTER 1

IDEAL KNOTS AND THEIR RELATION TO THE PHYSICS OF REAL KNOTS

ANDRZEJ STASIAK, JACQUES DUBOCHET
Laboratoire d'Analyse Ultrastructurale
Université de Lausanne
1015 Lausanne-Dorigny, Switzerland.
e-mail: Andrzej.Stasiak@lau.unil.ch
Jacques.Dubochet@lau.unil.ch

VSEVOLOD KATRITCH
Department of Chemistry
Rutgers the State University of New Jersey
New Brunswick, New Jersey 08903, USA.
e-mail: seva@dna2.rutgers.edu

PIOTR PIERANSKI
Department of Physics
Poznan University of Technology
Piotrowo 3, 60 965 Poznan, Poland
and
Institute of Molecular Physics,
Smoluchowskiego 17, 60 159 Poznan
e-mail: pieransk@phys.put.poznan.pl

We present here the concept of ideal geometric representations of knots which are defined as minimal length trajectories of uniform diameter tubes forming a given type of knot. We show that ideal geometric representations of knots show interesting relations between each other and allow us to predict certain average properties of randomly distorted knotted polymers. Some relations between the behaviour of real physical knots and idealised representations of knots which minimise or maximise certain properties were previously observed and discussed in Ref. 1-5.

1 Ideal knots

We learnt at school that the circle is the ideal planar geometric figure, since, amongst planar objects, it has the highest area to circumference ratio. Similarly the sphere is the ideal solid, since it has the highest volume to surface area ratio. The concept of ideal geometric objects was developed in Ancient Greece by Plato (427-347 B.C.), who said that we have the ability to intuitively grasp the ideal nature of those objects. Indeed intuition tells us, for example, that the equilateral triangle is the ideal triangle, and that the square is the ideal quadrilateral. Our intuition is corroborated by the fact that equilateral triangles and squares show the highest area to perimeter ratios for all triangles and quadrilaterals. Therefore, we can ask ourselves (as we would have asked Plato, given the chance) what are the ideal representations of different knots? Since knots occupy 3-D space, one should apply to them the principle of maximising their volume to surface area ratio. To attribute volume to knots in the most ideal way, one should consider them to be made of impenetrable cylindrical tubes of uniform diameter along their whole length. Obviously the highest ratio of the volume to surface area will be obtained for that configuration of the knot which allows us to minimise the length/diameter ratio of the tube forming a given type of knot.

One way to obtain ideal configurations is to uniformly increase the diameter of the cylindrical tube forming a knot while keeping the axial length constant and while adjusting the trajectory of the knot to permit the maximal radial inflation[3, 6]. Equivalently, one can proceed with shortening of the knotted cylindrical tube or rope while keeping its diameter constant until its length is minimised and the knot type is still maintained[7].

Fig.1 shows the process of rope shortening for the trefoil which initially has an arbitrary configuration. To begin with, axial shrinkage can take place everywhere and the axial trajectory of the knot therefore undergoes a simple scale reduction while the diameter of the rope remains unchanged. This leads to surface collisions of the rope segments, following which further shortening of the rope necessitates that its axial trajectory adjusts toward the ideal. Finally, further adjustments of the knot's trajectory and further shortening of the rope are not possible and we see that practically every radial crossection of the rope forming an ideal trefoil shows a point of contact with the surface of another segment of the rope. We intuitively feel that such maximally shortened trefoil knot showing a nice symmetry indeed adopts its ideal representation. The situation becomes less intuitive when using simulation approach we try to bring more complicated knots into their ideal configurations. Colour Plates 1-3 show the results of such simulations performed for all prime knots

with up to 8 crossings. The notations accompanying the knots shown correspond to Alexander-Briggs notations[8] used in standard tables of knots[9, 10] where the main number indicates the minimum number of crossings possible for this knot type and the index indicates the tabular position amongst the knots with the same minimum crossing number.

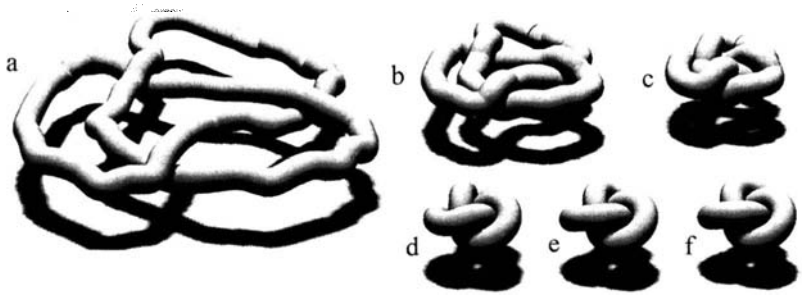

Fig. 1. Evolution of the trefoil knot towards its ideal conformation. The process of the knot tightening was simulated numerically with the SONO algorithm (see chapter by Pieranski). (a) - the initial conformation has an irregular shape. (b) to (e) - collisions between segments of the shrinking rope change its initial trajectory and allow maximal shortening of the whole rope. (f) - ideal conformation : the ratio of volume to surface area reaches its maximum.

It should be stressed here that the configurations presented are obtained by a simulation approach and it is still possible that they represent only a local rather than the absolute minimum in the configuration space of a given knot. We do not yet know how corrugated the conformational space of knots is or how many local minima and saddle points there are. We tested several different simulation algorithms in order to find procedures which are less likely to terminate in local minima. The algorithm used here (see chapter by Pieranski for its description) is less sensitive to local minima than the algorithm used previously to find ideal configurations of knots[6]. For example with the present algorithm we find that the symmetrical configuration of the knot 5_1; shown in Ref. 6 represents only a local minimum.

2 Ideal trajectories as knot invariants

Can the process of knot tightening be compared with finding a topological invariant of knots? If yes, then irrespective of the starting configuration of a given

knot, one should be able to obtain the same ideal configuration. Perhaps the best test for the knot tightening approach (and the computer algorithm used to simulate this process) is provided by the so-called Perko pair of knots. These two representations of 10 crossing knots were listed as distinct in knot tables compiled in 1899 by C.N. Little, and were believed by generations of topologists to correspond to different knot types, until, in 1974, K.A. Perko demonstrated that they represent the same knot. When Perko pair diagrams, denoted in Rolfsen tables as knots 10_{161} and 10_{162}, were taken as starting configurations for the process of knot tightening, the two configurations converged toward the same shape shown in Fig. 2.

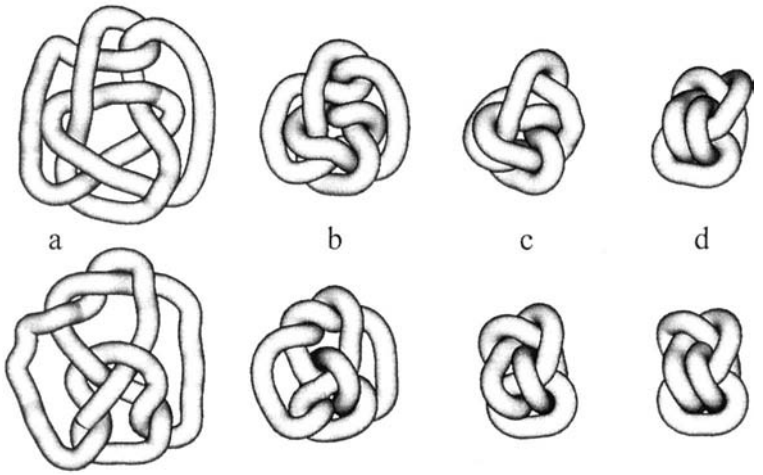

Fig. 2. Convergence of two different tabular representations of the Perko knot, into the same ideal form. (The final configurations of 10_{161} and 10_{162} are seen from slightly different angle)

3 Length/diameter ratio of ideal knots as a scale independent measure of the complexity of knots.

All knots shown in Plates 1-3 are constructed from rope of the same diameter. It is clear that as the knots become more complicated, one needs more rope to form the knot. To express the increasing complexity of ideal knots by a measure which is independent of the actual diameter of the rope, or the scale at which the ideal knot is presented, one can use the ratio of the length to the diameter of the rope forming a given ideal knot. Although we are not yet sure if our simulation approach will

always find the ideal configuration, it should be clear that one or more representation of a given knot exists for which the length to diameter ratio reaches the value of a global minimum. In the worst case there may be an infinite number of representations with the same length to diameter ratio but there will always be a length to diameter ratio value below which it is not possible to form a given knot. This minimum length/diameter ratio thus constitutes the topological invariant of a given knot. Of course without an analytical solution to the problem of ideal knots configurations we are limited in the precision of determination of the minimum length/diameter ratio. This is because our simulation approach is limited to polygonal knots made out of a limited number of segments of uniform size. However, we estimate that the error in the determination of the length to diameter ratio of ideal knots is less than 0.5%. Table I lists the length/diameter ratios obtained for different ideal knots.

The length to diameter ratio has a very simple intuitive meaning. It corresponds to the shortest relative length of very flexible but radially incompressible rope which is sufficient to tie a given type of knot. If one has, for example, a rope which is 1 cm thick, one would need at least 16.4 cm of this rope to form a trefoil (knot 3_1) and 47 cm to form knot 11_1: the more complicated the knot, the longer the piece of rope (of given diameter) required to tie it. A corollary is that the minimum length of rope needed to form a given knot should be a good measure of knot complexity. Knots could thus be classified and ranked according to the increasing length/diameter ratio of their ideal representations. Looking at Plate 3 and Table I we can see that the so-called nonalternating knots, which are placed in standard tables of knots as the last group of knots with a given minimum crossing number, e.g. 8_{19}, 8_{20}, 8_{21}, can be made with a piece of rope having a lower length/diameter ratio than alternating knots with the same minimum number of crossings. This result is easy to explain since in the alternating knots their trajectories are perfectly interwoven so that as we follow the rope forming ideal representations of alternating knots we see that it passes alternatively under and over the segments with which it crosses. In nonalternating knots the interweaving is not perfect and ropes can pass twice over and twice under the segments with which they cross and thus less rope is needed in-between such two crossings. Therefore, using as a criterion the length/diameter ratio of a rope forming the ideal representation of a given knot type, nonalternating knots are less complex than alternating knots with the same minimum crossing number. The fact that nonalternating knots can have shorter trajectories than alternating knots with the same minimum crossing number was observed also for strongly tightened knots made of real ropes (see the chapter by Janse van Rensburg) and for the minimum length knots on the cubic lattice[11](see also the chapter: "Minimal lattice knots" by Janse van Rensburg). Interestingly also

TYPE	L/D	ACN	Wr	TYPE	L/D	ACN	Wr
3_1	16.33	4.26	3.39	9_8	40.19	17.16	2.24
4_1	20.99	6.47	0.00	9_9	39.90	16.60	10.23
5_1	23.55	7.75	6.25	9_{10}	39.82	16.61	8.56
5_2	24.68	8.21	4.56	9_{11}	40.63	16.87	6.16
6_1	28.30	10.15	1.13	9_{12}	40.01	16.88	4.52
6_2	28.47	10.39	2.77	9_{13}	40.31	16.94	8.57
6_3	28.88	10.52	0.02	9_{14}	39.98	16.93	1.79
7_1	30.70	11.36	9.10	9_{15}	41.00	17.32	4.53
7_2	32.41	12.18	5.74	9_{16}	40.00	16.74	10.17
7_3	31.90	12.07	7.40	9_{17}	40.15	17.19	2.20
7_4	32.53	12.61	5.82	9_{18}	40.72	17.50	8.56
7_5	32.57	12.38	7.43	9_{19}	41.01	17.29	0.67
7_6	32.82	12.76	3.43	9_{20}	42.86	18.00	6.53
7_7	32.76	12.80	0.66	9_{21}	40.49	16.88	4.50
8_1	35.46	14.02	2.29	9_{22}	40.44	17.41	2.14
8_2	35.63	14.30	5.63	9_{23}	40.57	17.48	8.54
8_3	35.50	14.00	0.00	9_{24}	40.42	17.06	0.58
8_4	35.93	14.57	1.62	9_{25}	40.51	17.64	4.57
8_5	36.01	14.60	5.60	9_{26}	40.36	17.14	3.48
8_6	36.15	14.50	3.97	9_{27}	40.81	17.71	0.63
8_7	36.04	14.42	2.83	9_{28}	40.71	17.54	3.40
8_8	36.58	14.79	1.19	9_{29}	40.71	17.80	2.23
8_9	36.17	14.52	0.04	9_{30}	40.88	17.75	0.60
8_{10}	36.63	14.93	2.78	9_{31}	40.74	17.83	3.37
8_{11}	38.02	15.49	3.88	9_{32}	40.68	17.58	3.46
8_{12}	36.94	14.91	0.00	9_{33}	41.34	17.98	0.61
8_{13}	36.35	14.80	1.21	9_{34}	41.02	18.06	0.59
8_{14}	36.89	15.03	4.03	9_{35}	40.05	17.29	6.99
8_{15}	37.11	15.38	7.91	9_{36}	40.42	17.60	6.23
8_{16}	37.39	15.42	2.76	9_{37}	40.68	17.42	0.54
8_{17}	37.19	15.41	0.01	9_{38}	40.89	17.93	8.58
8_{18}	37.40	15.50	0.08	9_{39}	42.19	18.09	4.61
8_{19}	30.46	11.20	8.64	9_{40}	40.77	17.67	3.42
8_{20}	31.56	11.96	1.96	9_{41}	40.63	17.76	1.82
8_{21}	32.72	12.61	4.66	9_{42}	34.73	13.15	1.18
9_1	37.81	15.18	11.99	9_{43}	35.78	14.24	5.23
9_2	39.63	16.90	6.86	9_{44}	35.79	14.48	1.32
9_3	39.20	16.82	10.25	9_{45}	37.41	15.18	5.18
9_4	39.11	16.32	8.52	9_{46}	34.27	13.55	2.57
9_5	39.78	16.85	6.95	9_{47}	37.49	15.25	2.78
9_6	39.96	16.89	10.25	9_{48}	37.06	14.73	3.95
9_7	40.22	16.49	8.56	9_{49}	36.91	14.99	7.90

Table I Parameters of the most tight conformations found with the SONO algorithm.

the energies of nonalternating knots are smaller than the energies of alternating knots with the same minimal crossing number[2].

4 Average crossing number of ideal knots.

To characterise a knot one usually tries to find out what is the minimum number of crossings this knot can have in a planar projection. For example, there are 49 different prime knots which can be brought into configurations producing planar projections with the minimum number of crossings equal to 9, and all those knots are called 9 crossing knots. Minimum crossing number is by definition an integer and as such cannot be used for the fine distinction between different knots. Therefore as the minimum crossing number increases there are more and more knots with a given minimum crossing number (165 with 10 crossings). However, if instead of searching for the particular direction where a given knot shows minimum number of crossings one looks at the knot from infinitely many directions, one can calculate the average number of crossings which is a noninteger real number. Such a number, when calculated with high precision, can be uniquely attributed to the observed configuration of a given knot. Of course as long as we do not have unique representations of different knots, the value of the average crossing number will depend on the arbitrarily chosen configuration of a given knot. The situation is different for ideal knots which, at least in the case of not too complex knots tested by us, seemed to converge toward unique representations characteristic for a given type of knot. The average crossing number when calculated with high precision for the ideal configurations of knots is likely to be different for each knot type and as such can be used to distinguish between different knots. Table I lists the average crossing number calculated for the axial trajectory of ideal representations of different knots.

As with the length to diameter ratio of ideal knots, the average crossing number of the ideal configurations of knots is also a topological invariant. At the moment the only way to approach this value is by means of numerical simulations of limited precision, though elements of the analytical estimation have already been found (see chapter by Pieranski).

5 Relation between length/diameter ratio and the average crossing number of ideal representations of knots

When the values of the average crossing number of the ideal forms of 20 relatively simple knots (up to 11 crossings in their standard tabular representations) were plotted against the length/diameter ratio of the corresponding ideal forms, a quasi linear relation was obtained[6]. This prompted the question: is this relation strictly linear or is it a more complex one which only appears linear when relatively simple knots are taken into a consideration? Obviously the best way to answer this question is to take more complex knots, with minimum crossing numbers of several

dozens, and try to obtain their ideal configurations. However, as the knot becomes more complicated, the computer simulation gets more difficult and this increases the chances of obtaining final configurations which terminate in one of the local minima of the complex conformational space instead of the global minimum corresponding to the ideal configuration. In addition even if several independent simulation runs for the same knot type end in the same configuration we can not eliminate the possibility that there exists a better solution. Despite this uncertainty, we decided to simulate ideal trajectories of several more complex knots and to check their average crossing number and the length/diameter ratio. We have chosen torus type of knots for the simplicity of generation of their starting configurations.

Torus knots are defined as those which can be placed without self intersections on the surface of a regular torus. We took this class of torus knots which encircle twice the central straight axis of the torus and at the same time wind around the torus a given odd number of times. Since there are no tables of knots with more than 13 crossings other designations than the standard Alexander-Brigs notations are needed to describe more complicated knots. For torus type of knots the notation includes two numbers where the first one tells how many times the knot encircles the central straight axis of the torus and the second number tells how many times the knot winds around the torus (See (2,33)-torus knots on Fig. 3). Torus knots can be generated in nice symmetric configurations using a modified Lissajous approach where orthogonal oscillations are centred around a circular trajectory. Such symmetric torus knots evolve in an interesting way when they are used as the starting axial configurations for the simulation procedure (See Plate 4. and for more details see chapter by Pieranski). Initially the knots behave as if the tori about which knot axes wind were just getting thicker and shorter while the knots maintain a perfect cyclic group symmetry (C_{33} for the (2,33)-torus knot).

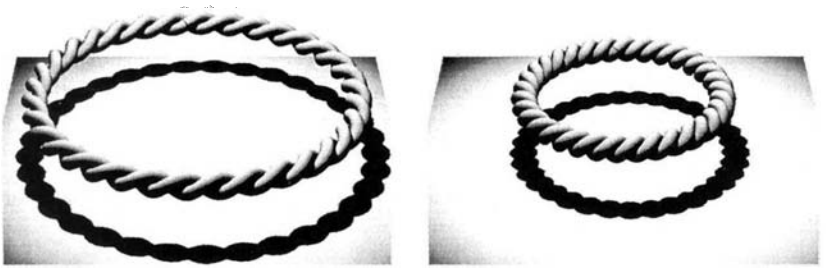

Fig. 3 The initial stage of evolution of the (2,33)-torus knot tightened with the SONO algorithm. For the next stages of the evolution see Plate 4.

Looking at the ropes forming symmetric torus knots one can see that they form a regular double helical arrangement whereby opposing ropes wind around a perfect circle.

During uniform shortening of the rope, axial paths of symmetric representations of torus knot change so that the opposing segments tend to become perpendicular to each other and then reach the optimum form (highest volume to surface area ratio) for this symmetric double helical arrangement (Fig 3b.) Further reduction in the rope length (maintaining fixed diameter) is only possible when the perfect double helical symmetry is broken and one of the opposing ropes becomes the central one. See Plate 4 and Fig. 4a. In this new arrangement the second, external rope can tightly wind around the central one. The symmetry breaking causes the whole knot to lose its toroidal shape upon which it folds into an irregular discoidal form whereby the opposing ropes switch between internal and external position in a non regular way.

In one of our long-duration simulation runs, a regular elongated form of torus knots emerged from the irregular discoidal form.

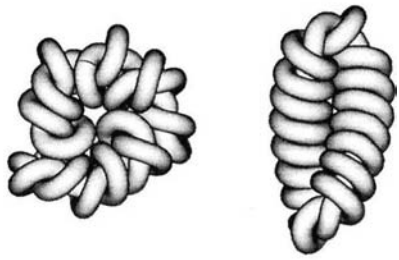

Fig. 4 Irregular discoidal and nice elongated form of (2,33)-torus knot obtained when starting from different initial configurations. See text and Plate 5.

In such elongated form there is only one place where the central and external rope exchange their positions (torus knots in contrast to torus links need to have a site where the central and external rope exchange). This site of rope exchange is located at one of the apexes of the elongated form (Fig. 4b and Plate 5). The elongated regular forms of torus knots with high crossing number demonstrated the shortest length, for a given rope diameter, of all the forms we have obtained. We assume therefore that these forms represent ideal configurations of torus knots. As seen in Plate 5, searching for the minimal rope length the elongated form becomes spontaneously twisted. Interestingly, for minimum length torus knots in the cubic lattice one also observes a tight winding of one strand around an essentially straight central strand (see Fig. 3 in the chapter "Minimal lattice knots" by Janse van Rensburg). As already indicated, our simulation procedure only rarely resulted in the generation of elongated regular forms when starting from the symmetric configurations of torus knots. However, when starting from configurations which were already constructed with one switch point between the external and central

rope, the simulations quickly reached a very regular elongated form with the shortest length for a given diameter (see the chapter by Pieranski). Therefore we were able to bring into this configuration very complex torus knots including (2,63)-torus knots and calculate their average crossing number and length/diameter ratios. Fig 5 shows the relation between the length/diameter ratio and the average crossing number of ideal representations of (2,n)-torus knots starting from the trefoil knot (2,3)-torus knot and ending with (2,63)-torus knot. It is visible that initial slope for less complex torus knots is lower than this for more complex torus knots. Therefore it seems that there is no universal linear relation between length/diameter ratio and average crossing number of ideal representations of all knots.

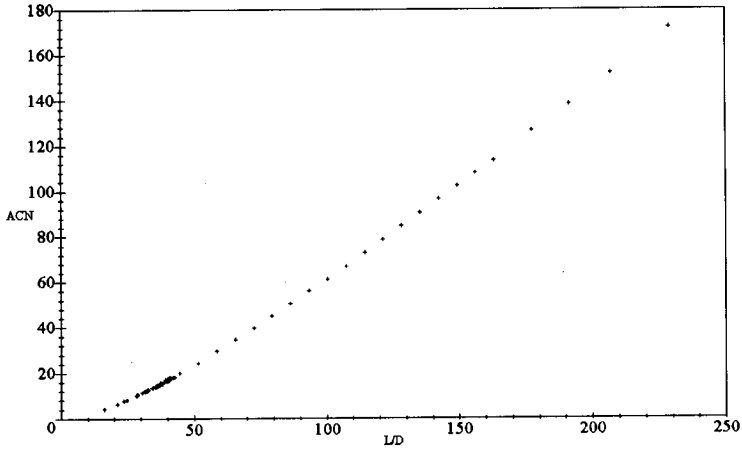

Fig 5. Relation between length/diameter ratio and average crossing number of the ideal geometrical representations of different knots, including the data obtained for large torus knots. Note a substantial change of the slope upon progression from simple toward more complicated knots.

However, as already mentioned, we are not sure that the elongated forms of large torus knots actually represent ideal forms of these knots. Furthermore we do not yet know if other large knots will follow the pattern of torus knots or if each family of knots will have its own characteristic relation between length/diameter ratio and the average crossing number of their ideal representations.

6 Writhe of ideal representations of knots.

Topologists are frequently interested in determining the chirality of different knots. Writhe is a measure of the chirality, and is quantified in a similar way as the mean crossing number. A given configuration of a knot is observed from thousands of directions, equisampling the sphere, and perceived crossings are counted.

However, in contrast to the mean crossing number, the chirality of the observed crossings is important. Thus, right handed crossings score as +1 and left handed as -1, and the writhe corresponds to the average score contributed by crossings perceived from a random direction, whereby the absolute writhe value is always smaller than the average crossing number. For achiral knots, the writhe of ideal configurations turned out to be practically equal to zero. Table I lists the writhe values calculated for ideal configurations of different knots. For chiral knots we provided writhe values of right-handed representations.

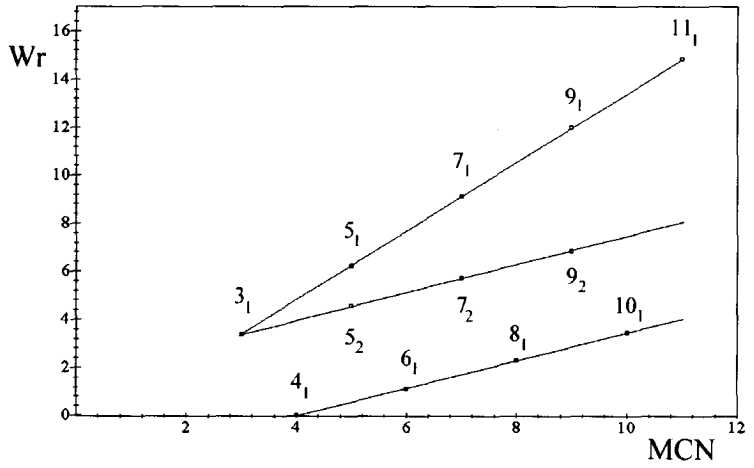

Fig 6. Different families of knots show different slopes of the linear increase of writhe Wr with increasing minimal crossing number (MCN). Knots 3_1, 5_1,...,11_1 belong to the family of the (2,n) torus knots. Knots 4_1, 6_1, 8_1 and 10_1 belong to the family of twist knots with the even number of crossings, while 3_1, 5_2, 7_2 and 9_2 belong to the family of twist knots with the odd number of crossings.

Fig. 6 shows that when the writhe values of ideal representations of different knots are plotted against their minimum crossing numbers, one observes a linear relationship between the knots belonging to the same families. So, for example, torus knots fell on one line with a characteristic slope while twist knots with even and odd numbers of crossings in their tabular standard representations are found on two parallel lines with a lower slope. Thus ideal representations of knots naturally divide themselves into families of knots and this division can be perceived without analysing the overall topology of the knots but just by measuring their writhe.

7 Ideal composite knots.

Composite knots are formed when two or more knots are tied successively on the same string. Composite knots can always be redistributed on a string in such a way that a plane pierced by the knot trajectory in only two places can separate the knot into two parts, whereby each part upon simple closure can form a nontrivial knot.

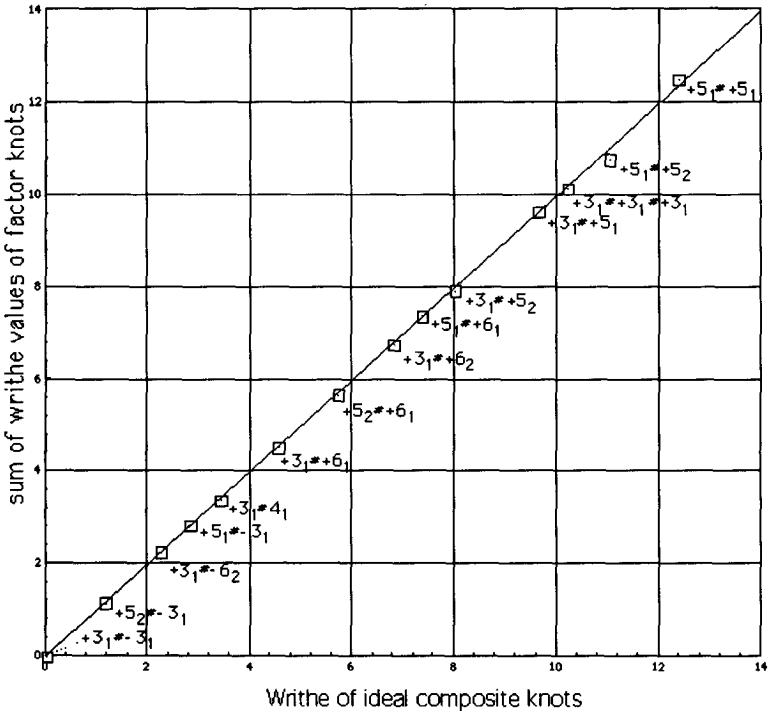

Fig. 7. Additivity of the writhe in composite knots.

Knots which constitute a composite knot are called factor knots. Of course the same criteria of ideality can be applied to composite knots as to the prime knots considered earlier. Plate 3 (lower part) presents the ideal configurations of some composite knots. Numerical notations indicate what factor knots are joined together to form a given composite knot, so for example $+3_1\#-3_1$ indicates that this composite knot is formed from one left and one right-handed trefoil (knot 3_1). Interestingly, the writhe of the ideal composite knot $+3_1\#-3_1$ turned out to be exactly zero as if positive writhe of a right-handed trefoil exactly compensated the negative

writhe of a left-handed trefoil (Table 2). Composite knot $+3_1\#-3_1$ is achiral[12] therefore our previous observation that the writhe of achiral prime knots in their ideal configurations is zero is apparently also valid for composite knots. When checking the writhe values for different composite knots in their ideal form we noticed that these values were always equal to the sum of the writhe values of the ideal forms of the factor knots constituting a given composite knot (Fig. 7). The observed additivity of writhe is a very interesting property of ideal knots since, usually, the writhe values are not additive[13] i.e. when one arbitrarily connects two closed curves in space by removing fragments of the original trajectories and replacing them by almost straight connectors, the writhe of the newly formed curve usually differs from the sum of the writhes of the two starting curves. It appears that factor knots, in the ideal forms of composite knots, adjust their trajectory and their relative position in respect to each other in such a way that upon joining of two or more ideal knots their total writhe does not change.

8 Relation between ideal and real trajectories of knots.

Upon discussing geometrical and topological relations between the ideal representations of different knots it is good to consider the connections between ideal and real knots. Perhaps we should recall here some thoughts of Plato, who said that although real objects do not have the properties of ideal objects, some reflection of ideality should still be present in real objects.

To look for the reflection of ideality in real knots it may be useful to consider the average shapes of thermally agitated knotted polymers in solution. In order to obtain reliable statistics it would be best to have a direct physical technique providing us with precise information about writhe and crossing number of the configurations actually adopted by millions of knotted molecules in solution. Although, at present, there is no such experimental technique, the progress in computer simulation techniques permits reliable generation and analysis of millions of expected configurations of knotted polymers in solution[14]. Certainly the most studied polymer is DNA, and we understand DNA properties sufficiently well to be able to use the Metropolis Monte Carlo simulation technique to model DNA behaviour under given conditions[15]. In order to have the shape of knotted DNA molecules unaffected by the intrinsic stiffness of DNA, we have chosen to model long DNA molecules so that the local curvature needed to form a given knot is usually smaller than the average local curvature induced by thermal motion. If modelled DNA molecules were short they would tend to minimise the curvature and would therefore systematically deviate from the equilibrium of stochastic representations satisfying the topology of a given knot. To eliminate the possible effects of torsional stress in double-stranded DNA we modelled DNA with interruptions in one of the strands so that torsional stress can dissipate. The

simulation results presented below refer to knotted double-stranded DNA molecules placed in a solution, though a qualitatively similar behaviour is expected for any torsionally relaxed knotted polymers suspended in a solution. Plate 6 shows a comparison between the axial trajectories of ideal knots and some modelled trajectories of knotted DNA molecules undergoing thermal motion. The modelled trajectories correspond to 5400 base pair-long DNA molecules forming a 3_1 and 4_1 knot, respectively. It is clear that the trajectories of the knotted molecules undergoing thermal motion bear little resemblance to the ideal trajectories of the corresponding knots. When the writhe is measured for momentary configurations of thermally shaken knotted molecules, the measured values very rarely approach those of the ideal configurations of the given knots. However, when the writhe is measured for millions of configurations, the mean value then becomes practically equal to the writhe of the ideal configuration. As shown in Fig. 8a this is true for the average writhe of every knot modelled, and is also true for different lengths of modelled DNA molecules.

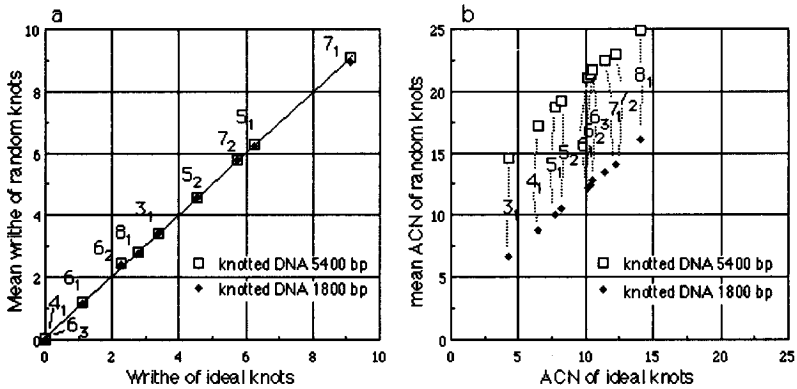

Fig. 8. Relations between ideal configurations of knots and knotted DNA chains undergoing thermal motion.

a. A 1:1 correspondence between the writhe of the ideal forms of knots and the mean writhe value of ensembles of ca. 9'000'000 configurations simulating the behaviour of knotted double-stranded DNA molecules (5400 and 1800 bp long) randomly distorted by thermal motion.

b. Linear correlation between the average crossing number of the ideal configurations and the mean of the average crossing numbers of ensembles of simulated configurations of knotted DNA chains with 1800 and 5400 base pairs.

The fact that the ideal configuration of a given knot has a writhe equal to the mean writhe of the floppy, randomly distorted polymers forming the same type of knot may initially be surprising. However, if one considers a simple circular polymer undergoing thermal motion one would expect that its momentary configurations can

be, with the same probability, twisted in right-handed and left-handed ways. Therefore the mean writhe, which is a measure of handedness or chirality should remain equal to 0, and a writhe of 0 is that of an ideal circle. Thus, for reasons of symmetry, floppy, circular polymers will maintain a mean writhe equal to that of an ideal circle. For the same reason floppy knots of different types will maintain their mean writhe equal to the writhe of the ideal configurations of these knots as long as the size of the knotted chains or of knotted domains is sufficiently large so that bending stress does not systematically change the shape of the knotted chains. Random knots built in the cubic lattice are free from bending stress and are ideal to test whether the mean writhe of a population of randomly distorted knotted chains forming a given knot corresponds to that of the ideal geometric representation of a given knot. Janse Van Rensburg *et al.* [16] calculated the mean writhe for randomly generated populations of different knots in the cubic lattice and noticed that for a given type of knot the mean writhe of the population did not depend on the number of segments in the walk. For example, populations of trefoils built of 24 segments or of 250 segments showed essentially the same writhe, 3.40±0.025, which corresponds to the writhe observed for ideal trefoils presented here. For more details concerning the mean writhe of random knots on the cubic lattice see the chapter by Janse van Rensburg, Sumners and Whittington.

Let us now look at the average crossing number of populations of knotted DNA molecules undergoing thermal motion. Fig. 8b shows that there is still a linear relationship between the average crossing numbers of ideal representations of different knots and the average crossing numbers calculated for populations of different knots with the same axial length. The slope of the observed linear relationship seems to be 1, and the longer the chain of the knotted polymers, the more additional crossings it has. Explaining the relationship between the average crossing numbers of the ideal representations of knots and those of a random population of knots one needs to point out the basic difference between the average crossing number and the writhe. Writhe is a measure of chirality so that additional crossings can have positive or negative values and, as discussed already, the accidental additional crossings have the same chance of adopting left or right handed configurations so that, on average, the contribution to writhe of additional crossings tends to 0. In contrast to the writhe, the average crossing number increases by +1 for each perceived crossing and thus additional crossings will never cancel each other but simply accumulate. The longer the polymeric chain undergoing thermal motion, the higher the number of additional crossings and this is exactly what is observed in Fig. 8b.

9 Gel electrophoresis as a physical method to test the relationship between ideal and real knots.

Upon observing 1:1 correspondence between the writhe of ideal knots and the mean writhe of modelled polymer chains forming corresponding knots one starts to appreciate that the ideal configurations predict or govern the real physical behaviour of knotted polymers in solution.

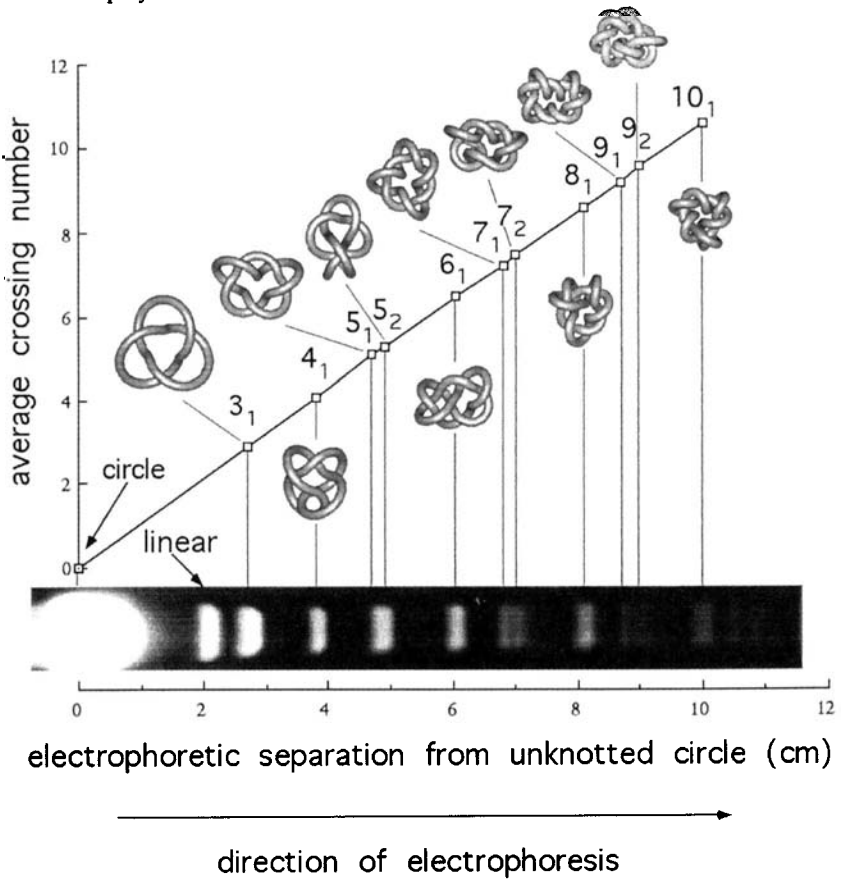

Fig. 9. Agarose gel electrophoresis separates DNA knots according to the overall compaction of ideal forms of the corresponding knots. The type of knot in each band was verified by electron microscopy. The ideal configuration of the corresponding knots were scaled to the same length and to facilitate visual tracing of the knots the diameter of the tubes was shrunk to 1/3 whilst maintaining the same axial path. The figure is adapted from Ref. 18

However, one may argue that the relationships described up to now are just between computer generated ideal configurations and computer generated random configurations of knots. A real physical test is needed. This test is provided by gel electrophoresis, a technique which can separate different DNA knots. In the laboratory of Nicholas Cozzarelli (University of Berkeley) this technique was brought close to perfection and Fig. 9 shows a gel where DNA molecules of the same length, though forming different well characterised knots, are analysed[17].

Ideal forms of different knots with the same length can be obtained by appropriate scaling of ideal knots with the same diameter but different length (as those shown on Plates 1-3). Upon correct scaling to bring different ideal knots to the same length we see that as knots become more complex their overall dimensions decrease (see corresponding representations of the knots in Fig. 9). The same applies to knotted DNA molecules of the same length, the more complicated the knot the more compact is the average configuration of this molecule. For molecules with the same charge, the higher the compaction the quicker the migration on the gel. Since the average crossing number is a good measure of knots compaction it is thus natural to plot the migration distance of different knots versus the mean crossing number of their ideal representations. Fig. 9 shows that this relation is linear. This demonstrates that the ideal configurations of knots can be used to predict the physical behaviour of real knots. It should, however, be mentioned here that knotted molecules on the gel do not adopt ideal configurations: but only their average shape has a compaction proportional to the compaction of ideal configurations of these knots.

10 Conclusions.

Ideal configurations of knots showed interesting geometrical and topological relationships between different knots. These configurations provide a basis for a natural classification of knots. Most importantly, however, is the fact that the physical behaviour of real physical knots can be predicted by the properties of the ideal representations of those knots. This was demonstrated here for polymers in solution but may also apply to other systems including superstrings on the lowest scale and cosmic strings on the highest.

Idealised representations of knots which minimise or maximise certain properties were shown to have interesting relations to the expected behaviour of real physical knots formed by magnetic flux lines[1], polymers[2,3], bistable chemical systems[4] or knotted fields[5]. (See also the chapters by some of the authors of these papers).

Several elements presented in this chapter were previously described in the Ref. 6,19-21.

Acknowledgements.

This work was supported by Swiss National Science Foundation grant 31-42158.94, Foundation Herbette, University of Lausanne, US public Health Service grants GM34809 and by Polish Scientific Committee grant 8T11-F010-08P04.

We thank Robert McNeel & Associates for providing us with the Rhinoceros Beta Release software with which most of the graphics presented in the chapter were created.

References

1. H. K. Moffatt, 1990, The energy spectrum of knots and links., *Nature* **347**, 367-369.

2. J. Simon, 1996, Energy functions for knots: beginning to predict physical behaviour., in *Mathematical Approaches to Biomolecular Structure and Dynamics* (eds. J. P. Mesirov, K. Shulten and D. W. Sumners) 39-58 (Springer-Verlag: New York).

3. A. Y. Grosberg, A. Feigel and Y. Rabin, 1996, Flory-type theory of a knotted ring polymer., *Phys. Rev. A* **54**, 6618-6622.

4. A. Malevanets and R. Kapral, 1996, Links, knots, and knotted labyrinths in bistable systems., *Phys. Rev. Lett.* **77**, 767-770.

5. L. D. Faddeev and A. J. Niemi, 1997, Stable knot-like structures in classical field theory, *Nature* **387**, 58-61.

6. V. Katritch, J. Bednar, D. Michoud, R. G. Scharein, J. Dubochet and A. Stasiak, 1996, Geometry and physics of knots., *Nature* **384**, 142-145.

7. P. Pieranski, 1996, Search of ideal knots, *ProDialog* **5**, 111-120 (in Polish).

8. J. W. Alexander and G. B. Briggs, 1927, On types of knotted curves, *Ann. of Math.* **28**, 562-586.

9. D. Rolfsen, 1976, *Knots and links* (Publish or Perish Press.: Berkeley, CA.).

10. C. C. Adams, 1994, *The Knot Book* (W.H. Freeman and Company: New York).

11. E. J. Janse van Rensburg, 1996, Lattice invariant for knots, in *Mathematical Approaches to Biomolecular Structure and Dynamics* (eds. J. P. Mesirov, K. Shulten and D. W. Sumners) 11-20 (Springer-Verlag: New York).

12. C. Liang and K. Mislow, 1994, On amphicheiral knots, *J. Math. Chem.* **15**, 1-34.

13. F. B. Fuller, 1978, Decomposition of the linking number of a closed ribbon: a problem from molecular biology, *Proc. Natl. Acad. Sci. USA* **75**, 3557-3561.

14. V. V. Rybenkov, N. R. Cozzarelli and A. V. Vologodskii, 1993, The probability of DNA knotting and the effective diameter of the DNA double helix, *Proc. Nat. Acad. Sci. U.S.A.* **90**, 5307-5311.

15. A. V. Vologodskii, S. D. Levene, K. V. Klenin, M. Frank-Kamenetskii and N. R. Cozzarelli, 1992, Conformational and thermodynamic properties of supercoiled DNA, *J. Mol. Biol.* **227**, 1224-1243.

16. E. J. Janse van Rensburg, E. Orlandini, D. W. Sumners, M. C. Tesi and S. G. Whittington, 1997, The writhe of knots in the cubic lattice., *Journal of Knot Theory and its Ramification* **5**, 31-44.

17. N. J. Crisona, R. Kanaar, T. N. Gonzalez, E. L. Zechiedrich, A. Klippel and N. R. Cozzarelli, 1994, Processive recombination by wild-type Gin and an enhancer-independent mutant. Insight into the mechanisms of recombination selectivity and strand exchange., *J. Mol. Biol.* **243**, 437-457.

18. A. V. Vologodskii, N. Crisona, B. Laurie, P. Pieranski, V. Katritch, J. Dubochet and A. Stasiak, 1998, Sedimentation and electrophoretic migration of DNA knots and catenanes, *J. Mol. Biol.* **278**, 1-3.

19. A. Stasiak, V. Katritch, J. Bednar, D. Michoud and J. Dubochet, 1996, Electrophoretic mobility of DNA knots, *Nature* **384**, 122.

20. A. Stasiak, 1997, Nœuds idéaux et nœuds réels, *Pour la Science, special issue: La Science des Nœuds* **April 1997**, 106-111.

21. V. Katritch, W. K. Olson, P. Pieranski, J. Dubochet and A. Stasiak, 1997, Properties of ideal composite knots, *Nature* **388**, 148-151.